ACS OMEGA

Open Access

http://pubs.acs.org/journal/acsodf

Article

Adsorption Behavior of Dissolved Gas Molecules in Transformer Oil on Rh Modified GeSe Monolayer

Yunfeng Long, Zhaoyu Peng, Liang-Yan Guo,* Xiaohui He, Mengyao Zhu, Zewen Yang, and Taiwen Liu

Cite This: *ACS Omega* 2024, 9, 7061−7068

Read Online

ACCESS | Metrics & More | Article Recommendations

ABSTRACT: Dissolved gas analysis in transformer oil is useful for detecting early transformer failures. The research on gas sensors for monitoring dissolved gas in transformer oil has attracted wide attention from academia and industry. In this study, Rh-doped GeSe monolayers were used as gas sensing materials based on the density functional theory (DFT). The potential of the Rh-GeSe monolayer as a gas sensor was evaluated by calculating the geometric structure, adsorption distance ($d_{sub/gas}$), binding energy (E_b), adsorption energy (E_{ads}), transfer charge (ΔQ), the density of states (DOS), band structure, electron localization function (ELF), charge difference density (CDD), and sensitivity (S) of Rh-GeSe monolayer with eight gas molecules (SO_2, C_2H_2, NO_2, H_2, CH_4, CO_2, H_2S, and CO). The results show that the Rh-GeSe monolayer has a prominent response to SO_2, C_2H_2, and NO_2 gas molecules and has great potential to become an excellent gas sensor. This study provides a theoretical basis for the application of Rh-GeSe monolayer in the field of gas sensing and provides a new way for the development of other gas sensors.

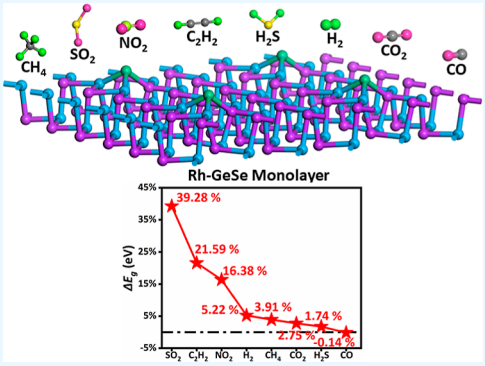

1. INTRODUCTION

As one of the main equipment in the power system, the normal operation of the transformer is crucial for the reliability and stability of the power system.[1] Dissolved gas analysis (DGA) in oil[2] is an effective means to find early transformer faults and can determine the operating status of the transformer in advance,[3,4] which is of great significance in guiding the transformer overhaul work and preventing major accidents in the power grid.[5−7] Overheating of oil and paper inside the transformer, partial discharge of oil-paper insulation, moisture or bubbles in the oil, increased water content in the oil, and so forth will produce H_2, CH_4, NO_2, C_2H_2, CH_4, and other dissolved gases in the oil.[8−10] DGA can monitor the dissolved gas in the transformer oil in real time and online and send out an alarm signal when the concentration and rate of change of the dissolved gas in the oil exceeds a certain limit, so that effective measures can be taken in time to avoid transformer failure.[11,12] Therefore, the effective monitoring of dissolved gases in transformer oils is of great significance.

As a new gas monitoring technology, gas sensors are applied to dissolved gases in transformer oil decoration, industrial production, exhaust emissions, and other fields to monitor various toxic and harmful gases.[13,14] The gas sensor can intuitively display the information on the type, concentration, and flow rate of the target gas as the corresponding resistance or voltage value of the gas sensing material after the physical and chemical reaction with the measured gas.[15,16] According to the change of resistance or voltage caused by the physical and chemical reaction between the gas sensing material and the measured gas, the corresponding actual situation can be obtained by calculation so as to achieve the effect of monitoring, control, and early warning. Therefore, as the core component of gas sensors, the development of gas sensing materials is the key means to improving the performance, reducing the cost, and upgrading the technology of gas sensors.

With the development of nanotechnology, nanoelectronic materials are playing an indispensable role in the field of gas sensing. According to the dimension classification, nanoelectronic materials can be divided into low-dimensional structures (zero-dimensional, one-dimensional, two-dimensional) and high-dimensional structures (three-dimensional).[17−20] Among them, two-dimensional nanoelectronic materials such as graphene, boron nitride, molybdenum disulfide, and germanium selenide have become a research hotspot in the field of gas sensing due to their large specific surface area, excellent electrical properties, and excellent mechanical properties.[21−26] These two-dimensional nanoelectronic materials have strong interactions with the adsorbed gas, making their electrical properties more susceptible to physical or chemical adsorption. Among them, GeSe as a new

Received: November 12, 2023
Revised: January 13, 2024
Accepted: January 22, 2024
Published: January 31, 2024

https://doi.org/10.1021/acsomega.3c09001
ACS Omega 2024, 9, 7061−7068

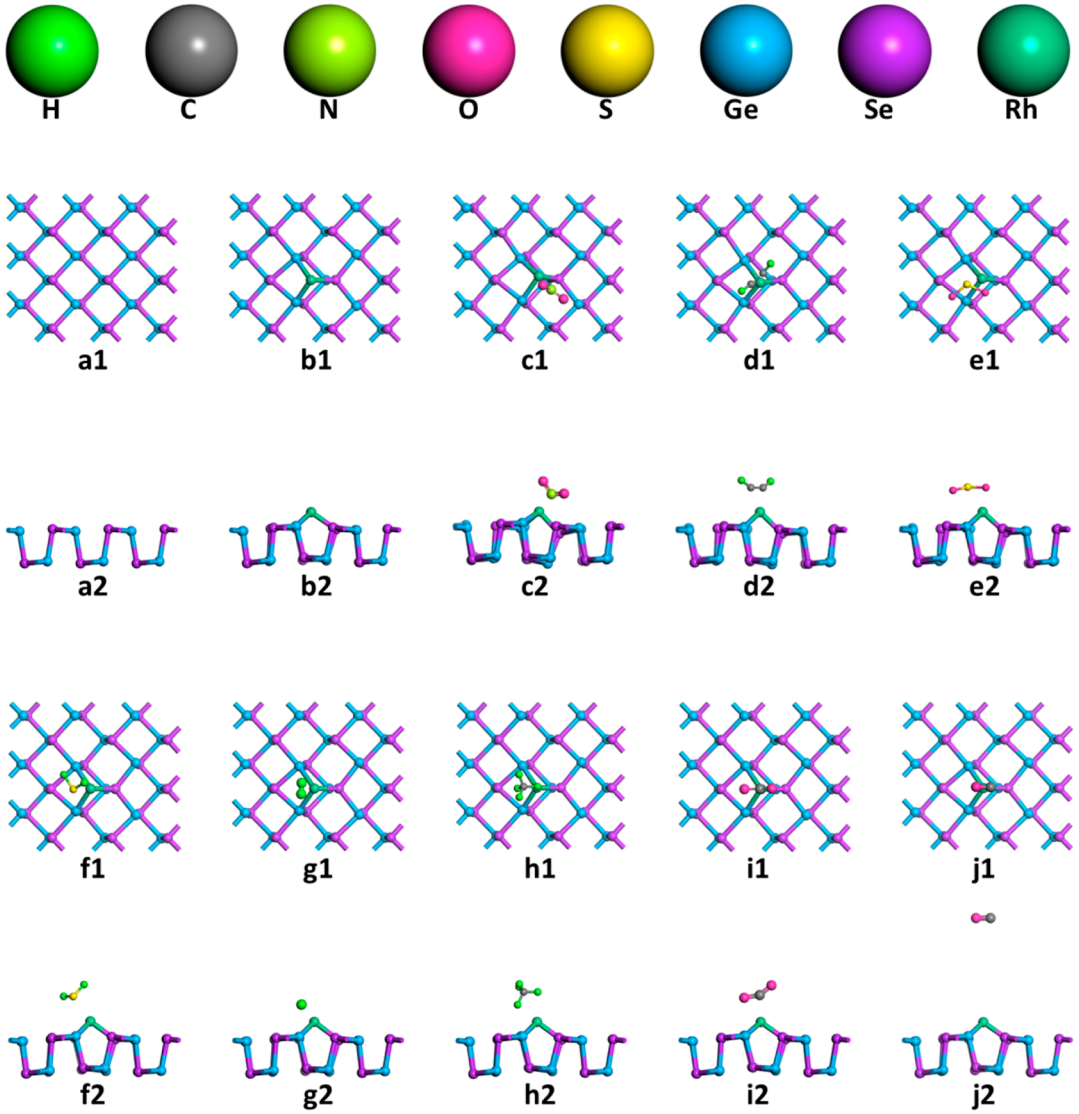

Figure 1. Geometric structures of (a1,a2) GeSe monolayer, (b1,b2) Rh-GeSe monolayer, and (c1,c2) NO_2, (d1,d2) C_2H_2, (e1,e2) SO_2, (f1,f2) H_2S, (g1,g2) H_2, (h1,h2) CH_4, (i1,i2) CO_2, and (j1,j2) CO adsorption systems.

p-type semiconductor with about 1.0 eV has attracted the attention of researchers in the field of gas sensing.[27−29] In addition, GeSe also has the advantages of good stability, abundant reserves, and no pollution to the environment, which can become a large-scale prepared gas sensing material for the future.[30−32] However, due to the limitation of physical and chemical properties of intrinsic GeSe, its gas sensing monitoring sensitivity is low, the gas sensing response speed is slow, and the selectivity is poor. To solve the above problems, researchers used a variety of physical and chemical methods, including mechanical deformation, organic functional group modification, and metal modification, to modify its microstructure to improve its gas sensing properties.[33−36] Among them, the noble metal doping method can effectively improve the response value and selectivity of gas sensing materials by reducing the reaction energy barrier between gas sensing and the target gas and increasing the percentage of activated molecules. However, GeSe is still in the development stage, and doping it through experiments will cost more manpower, material, and financial resources. Environmental pollution and energy consumption caused by this process are irreversible. Therefore, theoretical simulation can effectively reduce the blindness of the experiment, save a lot of time, and provide strong guidance for the preparation of the corresponding gas sensors in the later stage.

In this study, based on the density functional theory (DFT), the GeSe monolayer model doped with Rh atom was established with GeSe as the substrate material, and the adsorption characteristics of eight gas molecules (SO_2, C_2H_2, NO_2, H_2, CH_4, CO_2, H_2S, CO) were studied theoretically. Through the analysis of geometric structure, adsorption distance ($d_{sub/gas}$), binding energy (E_b), adsorption energy (E_{ads}), transfer charge quantity (ΔQ), the density of states (DOS), band structure, electron localization function|electron local function (ELF), charge difference density (CDD), and sensitivity (S), the interaction between Rh-GeSe monolayer and target gas molecules was clarified, and the value of Rh-GeSe monolayer in gas sensing field was evaluated based on this.

https://doi.org/10.1021/acsomega.3c09001
ACS Omega 2024, 9, 7061−7068

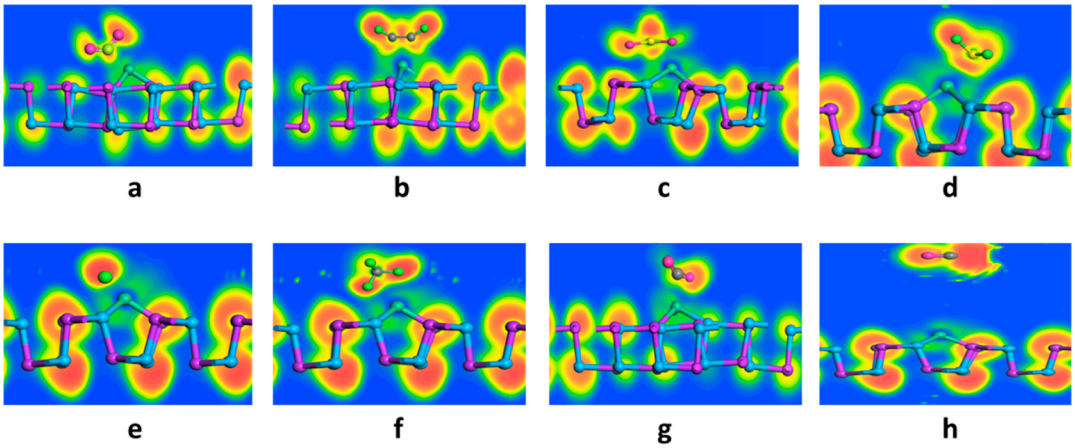

Figure 2. ELF of (a) SO_2, (b) C_2H_2, (c) NO_2, (d) H_2, (e) H_2S, (f) CH_4, (g) CO_2, and (h) CO adsorption systems.

2. COMPUTATIONAL DETAILS

Based on DFT, all theoretical calculations are performed in Materials Studio. Perdew−Burke−Ernzerhof (PBE) and double numerical polarization of the generalized gradient approximation are used for the exchange−correlation functional and basis set, respectively. Kernel electronics are processed by the DFT semicore pseudopots (DSPP) method. The influence of the van der Waals force is corrected by the DFT-D method based on Grimme. For the charge transfer between gas molecules and the Rh-GeSe monolayer, the Mulliken population was chosen to calculate. The Monkhorst−Pack, energy convergence accuracy, vacuum layer, maximum stress, and maximum displacement were set to $6 \times 6 \times 1$, 1×10^{-6} Ha, 20 Å, 2×10^{-3} Ha/Å, and 5×10^{-3} Å, respectively. First, the molecular models of NO_2, C_2H_2, SO_2, H_2S, H_2, CH_4, CO_2, and CO were established, and the structural optimization calculation was carried out to ensure the stability of the gas molecular structure and closer to the actual situation. Meanwhile, a $4 \times 4 \times 1$ GeSe supercell model with 18 Ge atoms and 18 Se atoms is established. Then, Rh atoms are placed near the GeSe surface from different angles and distances and optimized to obtain the most stable Rh-GeSe monolayer. Specifically, the Rh-GeSe monolayer model is constructed by placing Rh atoms above the center of the hexagonal pore, above Ge atoms, above Se atoms, and above the midpoint of the Ge−Se bond. Finally, the adsorption models of SO_2, C_2H_2, NO_2, H_2, CH_4, CO_2, H_2S, and CO gas molecules on the Rh-GeSe crystal surface were established according to different orientations and the most stable adsorption structure and various adsorption parameters. In the process of building the adsorption model, the possible situations in actual adsorption are taken into account as much as possible to avoid the influence of random adsorption sites and gas molecular orientation on the research. In addition, the study considers the effect of humidity changes on sensor performance.

3. RESULT AND DISCUSSION

In order to determine the optimal structure of the Rh atom doped GeSe monolayer, the binding energies of various coordinations were calculated. In this study, the binding energy formula of the Rh-doped GeSe monolayer is

$$E_b = E_{Rh-GeSe} - E_{GeSe} - E_{Rh} \quad (1)$$

where $E_{Rh\text{-}GeSe}$, E_{GeSe}, and E_{Rh} represent the energy of Rh-GeSe monolayer, pristine GeSe monolayer, and Rh atom, respectively. When the binding energy is negative, this indicates that the doping reaction is exothermic and can be carried out spontaneously. The larger absolute value indicates that the more stable the Rh-GeSe monolayer formed by this method, the more likely it is to be the gas sensing material obtained in the experimental preparation. After calculation and comparison, the minimum binding energy of Rh-GeSe monolayer doping is −4.249 eV. The Ge−Se bond length near the doping site only decreases from 2.616 to 2.588 Å. The percentage of bond angle change is smaller. The small geometric structure change after doping is the basis of the stability of gas sensing materials, as shown in Figure 1a1,b1. The doped Rh atom is located on the surface of the GeSe monolayer. The newly formed Rh−Se bond length and Rh−Ge bond length are 2.373 and 2.362 Å, respectively. The appropriate position and the appropriate bond length of the new bond are more conducive to the adsorption reaction between the Rh-GeSe monolayer and gas molecules, thus showing a moderate resistance value change or voltage value change macroscopically. Therefore, the subsequent calculation of the adsorption system was based on the Rh-GeSe monolayer. In order to obtain the most stable adsorption system, NO_2, C_2H_2, SO_2, H_2S, H_2, CH_4, CO_2, and CO molecules are close to Rh-GeSe monolayer at different initial positions. Figure 1c1−j2 showed the most stable geometric structure of the above adsorption system. After the most stable adsorption system was obtained, a series of physical and chemical parameters characterizing the optimized structure were introduced to analyze the adsorption process of the Rh-GeSe monolayer on gas molecules. Adsorption distance ($d_{sub/gas}$) represents the nearest distance between the Rh-GeSe monolayer and gas molecules; adsorption energy (E_{ads}) represents the force of gas molecules adsorbed on the Rh-GeSe monolayer surface; ELF is used to characterize the localization degree of electrons in the adsorption system. In this study, the calculation formula of adsorption energy (E_{ads}) is

$$E_{ads} = E_{Gas/Rh-GeSe} - E_{Gas} - E_{Rh-GeSe} \quad (2)$$

where $E_{Gas/Rh\text{-}GeSe}$, E_{Gas}, and $E_{Rh\text{-}GeSe}$ represent the energy of adsorption systems, gas molecule, and Rh-GeSe monolayer, respectively. The adsorption energies of the most stable adsorption systems of NO_2, C_2H_2, SO_2, H_2S, H_2, CH_4, CO_2, and CO are −2.009 eV, −1.656 eV, −1.630 eV, −1.183 eV,

https://doi.org/10.1021/acsomega.3c09001
ACS Omega 2024, 9, 7061−7068

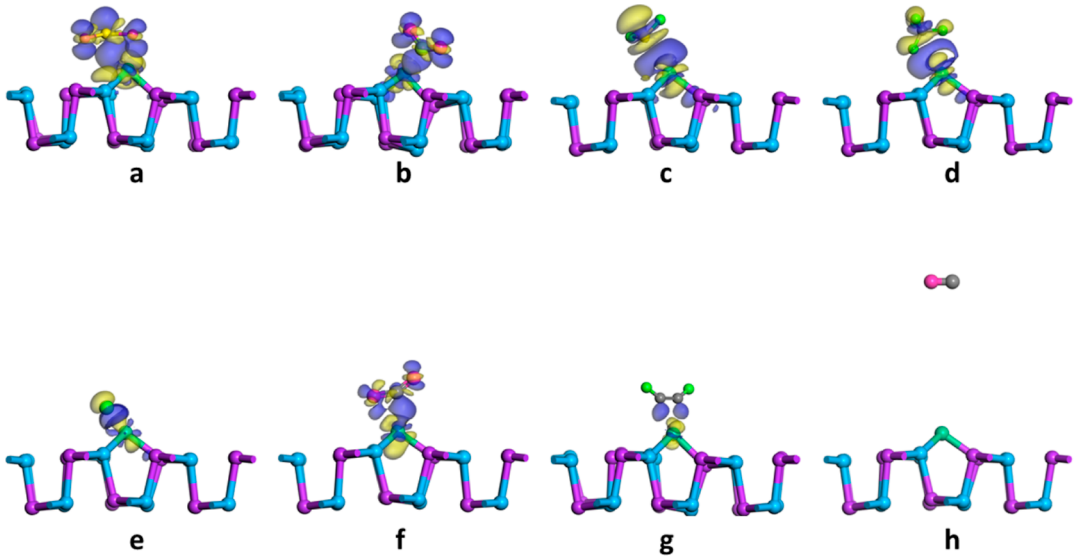

Figure 3. CDD of (a) SO_2, (b) NO_2, (c) H_2S, (d) CH_4, (e) H_2, (f) CO_2, (g) C_2H_2, and (h) CO adsorption systems.

−0.817 eV, −0.448 eV, −0.308 eV, and −0.059 eV, respectively. The adsorption reaction is usually accompanied by a change in the system energy. According to the energy change of the system, the adsorption reaction can be divided into exothermic and endothermic reactions. According to Formula 2 and the calculation results, the adsorption energies of the adsorption systems in this study are all negative, namely, they are all exothermic reactions. The exothermic reaction refers to the adsorption reaction accompanied by an energy release. The total energy of the adsorbed system is less than that of gas molecules and the Rh-GeSe monolayer before adsorption. This means that the adsorption reaction between the Rh-GeSe monolayer and the above eight gases does not require external energy absorption and can be carried out spontaneously. Smaller adsorption can indicate that the Rh-GeSe monolayer reacts strongly with NO_2, C_2H_2, SO_2, H_2S, and H_2 gas molecules. The adsorption energies of NO_2, C_2H_2, SO_2, H_2S, and H_2 adsorption systems are less than −0.6 eV. According to previous experience, these adsorption reactions can be considered as chemical reactions.

However, according to the ELF, the adsorption of NO_2, C_2H_2, SO_2, H_2S, and H_2 adsorption systems is more likely to be between physical adsorption and chemical adsorption, as shown in Figure 2a−e. The green region between Rh-GeSe monolayer and gas molecules in NO_2, C_2H_2, SO_2, H_2S, and H_2 adsorption systems tends to fuse obviously, but the orange region is obviously different from that between bonding atoms. This indicates that the adsorption of these five adsorption systems is strong but not sufficient to form stable chemical bonds. This indicates that these adsorption systems have moderate adsorption effects. Moderate adsorption is the key to the excellent cycling performance of gas sensing materials. This is because moderate adsorption is beneficial for the adsorption and desorption of gas molecules. Figure 2f−h shows an obvious blue region between CH_4, CO_2, CO gas molecules, and Rh-GeSe monolayer. This indicates that the adsorption intensities of these three adsorption systems are obviously small. Especially in the CO adsorption system, the blue region is significantly different from the other seven adsorption systems. This is consistent with the adsorption energy of the CO adsorption system being only −0.059 eV. Such a small adsorption energy means that the interaction between gas molecules and gas sensing materials is very weak, which is not conducive to the change of electrical parameters of the Rh-GeSe monolayer. This is also reflected in the calculation results of the adsorption distance (d_{sub}/gas). The distance between the Rh atom and the C atom in the CO gas molecule is 8.256 Å, which is much larger than that between other gas molecules and the Rh-GeSe monolayer. The adsorption system of NO_2, C_2H_2, SO_2, H_2S, and H_2 between physical adsorption and chemical adsorption is not strong, which means that there is no large energy barrier in this adsorption process, which is conducive to the desorption of gas. This indicated that from the perspective of adsorption intensity, the adsorption systems of NO_2, C_2H_2, SO_2, H_2S, and H_2 were relatively moderate. It is worth noting that the adsorption energies of different adsorption systems are obviously different, and the adsorption energy of the NO_2 adsorption system is 34 times that of the CO adsorption system. This indicates that the Rh-GeSe monolayer has strong selectivity for the above gases. Therefore, from the perspective of adsorption energy, adsorption distance, and ELF, the Rh-GeSe monolayer can effectively distinguish and monitor NO_2, C_2H_2, SO_2, H_2S, and H_2 gases.

In the gas adsorption reaction, in addition to obvious changes in the system energy, a large number of electron exchanges will also be generated. Therefore, in order to provide more theoretical support for the intensity of the adsorption reaction or the type of physical and chemical reactions, this study also calculated the charge transfer and CDD. Transfer charge quantity (ΔQ) reflects the change of charge quantity between Rh-GeSe monolayer and gas molecules during adsorption; the CDD can better explain the charge transfer mechanism. In this study, the calculation formula of charge transfer is

$$\Delta Q = Q_a - Q_b \tag{3}$$

where Q_a and Q_b represent the total charge of gas molecules after and before adsorption, respectively. The transfer charges of the most stable SO_2, NO_2, H_2S, CH_4, H_2, CO_2, C_2H_2, and CO adsorption systems were −0.405 e, −0.274 e, −0.22 e, 0.164 e, 0.157 e, −0.142 e, 0.047 e, and −0.001 e, respectively. From the point of view of the transfer charge, except for the

https://doi.org/10.1021/acsomega.3c09001
ACS Omega 2024, 9, 7061−7068

CO and C_2H_2 adsorption systems, the transfer charge of other adsorption systems is larger. In particular, the transfer charge of the SO_2 adsorption system was 405 times that of the CO adsorption system. A large transfer charge means that the Rh-GeSe monolayer has a high sensitivity to SO_2. According to the calculation results, in the SO_2, NO_2, H_2S, CO_2, and CO adsorption system, the Rh-GeSe monolayer transfers electrons to gas molecules. In CH_4, H_2, and C_2H_2 adsorption systems, gas molecules transfer electrons to the Rh-GeSe monolayer.

Figure 3 shows charge transfer in the adsorption reaction. Among them, the blue region represents the electronic dissipation area, and the yellow region represents the electronic gathering area. It can be clearly seen that the charge transfer of the SO_2, NO_2, H_2S, CH_4, H_2, and CO_2 adsorption system is particularly intense, as shown in Figure 3a–f. In the SO_2 adsorption system, there is a large electron concentration area around the S and the O atoms, as shown in Figure 3a. This indicated that SO_2 gas acted as an electron acceptor and the Rh-GeSe monolayer acted as an electron donor in the SO_2 adsorption reaction. This is consistent with the transfer charge calculated previously. In addition, a large number of electron dissipation regions and electron concentration regions are centered between the SO_2 gas molecules and Rh atoms. This indicates that the charge transfer mainly occurs between SO_2 gas molecules and the Rh-GeSe monolayer, and the charge transfer is quite intense. In the C_2H_2 adsorption system, there is a small electron dissipation region around the C atom and a small electron aggregation region around the Rh atom, as shown in Figure 3g. This indicates that in the C_2H_2 adsorption reaction, C_2H_2 gas molecules act as electron donors and the Rh-GeSe monolayer acts as electron acceptor. This is also consistent with the transfer charge of the previous C_2H_2 adsorption system (ΔQ = 0.047 e). A small amount of electron concentration area and electron dissipation area also means that the change of macroscopic resistance or voltage value caused by the C_2H_2 adsorption system will be significantly different from that of the SO_2 adsorption system. These phenomena demonstrate once again that the Rh-GeSe monolayer has strong selectivity for the above gases.

To further study the adsorption mechanism, the total density of states (TDOS) of GeSe monolayer, Rh-GeSe monolayer, and SO_2, C_2H_2, NO_2, H_2, CH_4, CO_2, H_2S, and CO gas adsorption systems were calculated, as shown in Figure 4. In the TDOS distribution of the GeSe monolayer and Rh-GeSe monolayer, the TDOS after doping obviously shifts to the left and has a great chance near the Fermi level, as shown in Figure 4a. These changes are due to the orbital hybridization and charge transfer in the Rh atom doping process. This means that the introduction of Rh atoms will make the substrate material more stable. In the TDOS distribution of SO_2, C_2H_2, NO_2 adsorption system, TDOS has changed greatly before and after adsorption, especially near the Fermi level, there are obvious right shifts and some new peaks appear, as shown in Figure 4b–d. This is due to the obvious adsorption reaction between SO_2, C_2H_2, NO_2 gas molecules, and Rh atoms, and the state peaks of their orbitals move, split, or merge to varying degrees, which makes TDOS change greatly. These TDOS changes are moderate. This also proves again that the three adsorption systems mentioned above are between physical and chemical adsorption. For the adsorption system, especially for the CO adsorption system, before and after adsorption on the Rh-GeSe monolayer, there is no obvious change in the electron filling probability of TDOS near the Fermi level, but there is

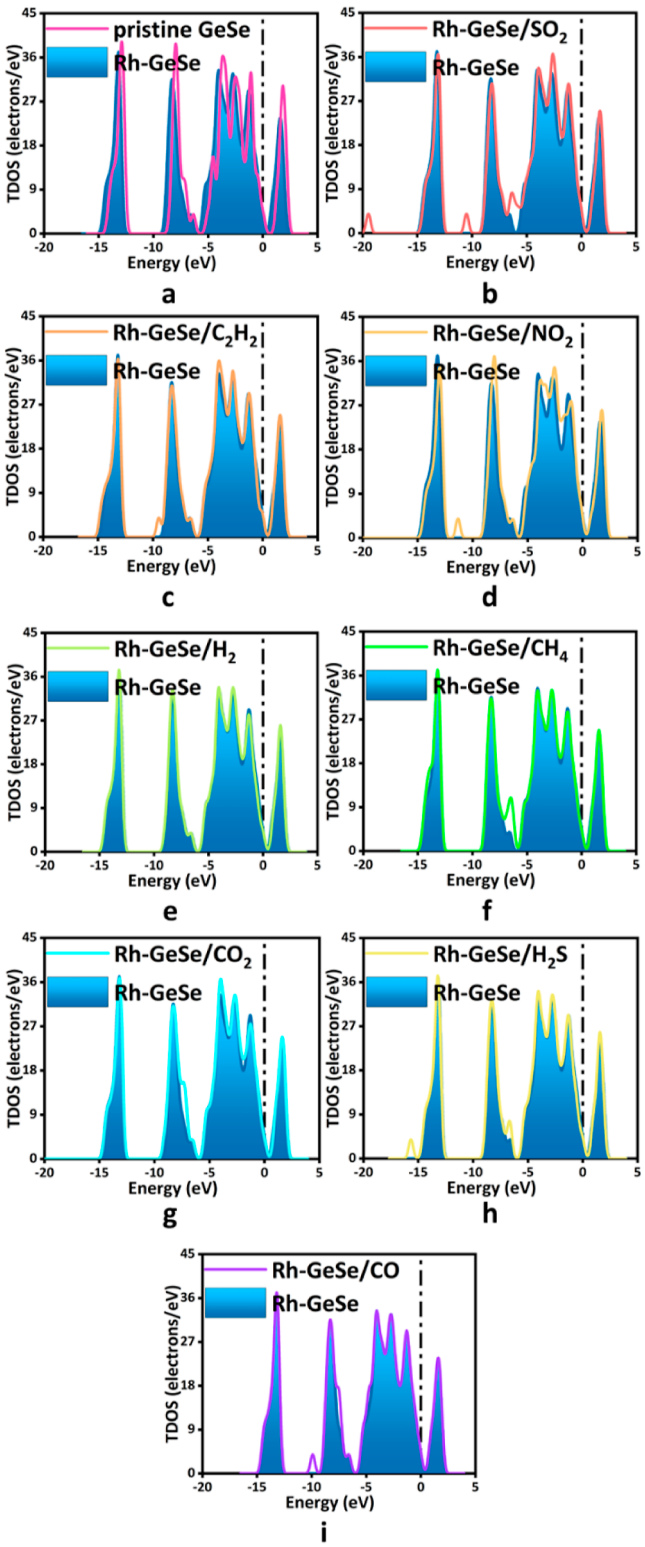

Figure 4. TDOS of (a) GeSe monolayer and Rh-GeSe monolayer, (b) SO_2, (c) C_2H_2, (d) NO_2, (e) H_2, (f) CH_4, (g) CO_2, (h) H_2S, and (i) CO adsorption systems.

only a new peak near far below the Fermi level, as shown in Figure 4e–i. However, this does not contribute to the change of conductivity, which is also consistent with the smaller adsorption energy, smaller charge transfer, and farther adsorption distance of CO molecules in the adsorption process. This is mainly caused by the weak physical adsorption

https://doi.org/10.1021/acsomega.3c09001
ACS Omega 2024, 9, 7061−7068

of the adsorption reaction. Therefore, from the perspective of TDOS, Rh-GeSe monolayer has obvious monitoring effect on SO_2, C_2H_2, and NO_2 gas molecules.

In order to further study the electronic properties in the adsorption process, the band structures of GeSe monolayer, Rh-GeSe monolayer, and SO_2, C_2H_2, NO_2, H_2, CH_4, CO_2, H_2S, and CO gas adsorption systems were calculated, as shown in Figure 5. After doping with Rh, the band gap energy of the GeSe monolayer decreases from 1.007 to 0.690 eV. This indicates that the band gap is reduced due to the doping of Rh atoms. This means that when the target gas contacts the Rh-GeSe monolayer, the transition of electrons from a low level to a high level requires less energy, which is more likely to cause the change of conductivity. Therefore, the doping of Rh atoms causes the electrical and physical properties of GeSe monolayers to change in favor of gas sensing.

Figure 5c–e shows the band structure of the SO_2, C_2H_2, and NO_2 adsorption systems. It can be seen from the energy band diagram that a new energy level is introduced near the Fermi level, indicating that the reaction of the Rh-GeSe monolayer with SO_2, C_2H_2, and NO_2 gas molecules is stronger. This also means that Rh-GeSe monolayer adsorption of SO_2, C_2H_2, and NO_2 before and after will produce changes in conductivity greater than those of other adsorption systems. In addition, after adsorption of SO_2, C_2H_2, NO_2, H_2, CH_4, CO_2, and H_2S gas molecules, the band gap energy of the system increases, which means that the conductivity of the system decreases after adsorption. After CO gas molecules are adsorbed, the band gap energy of the system decreases, which means that the conductivity of the system increases after the adsorption of CO gas adsorption. In order to further compare the band gap energy of each adsorption system, the change rate was calculated, as shown in Figure 5k. In this study, the calculation formula of band gap energy (ΔE_g) is as follows

$$\Delta E_g = [(BG_{gas/Rh-GeSe} - BG_{Rh-GeSe})/BG_{Rh-GeSe}] \times 100\% \quad (4)$$

where $BG_{Gas/Rh-GeSe}$ and $BG_{Rh-GeSe}$ represent the band gap energy of adsorption systems and the Rh-doped GeSe monolayer, respectively. Obviously, the SO_2, C_2H_2, and NO_2 adsorption systems have more obvious band gap energy change than their adsorption system. In order to further explore the practicability of the Rh-GeSe monolayer, the sensitivity of each adsorption system was calculated. In this study, the calculation formula of sensitivity (S) is as follows

$$\sigma \propto \exp(-E_g/2kT) \quad (5)$$

$$S = (1/\sigma_{gas/Rh-GeSe} - 1/\sigma_{Rh-GeSe})/(1/\sigma_{Rh-GeSe}) \quad (6)$$

where k and T represent Boltzmann constant (1.38×10^{-23} J/K) and thermodynamic temperature, respectively. The $\sigma_{gas/Rh-GeSe}$ and $\sigma_{Rh-GeSe}$ represent the electrical conductivity of the gas adsorption system and the electrical conductivity of the Rh-GeSe monolayer, respectively.

Figure 6 shows the sensitivity of each adsorption system at 298, 348, and 398 K. At 298 K, the response values of Rh-GeSe monolayer to SO_2, C_2H_2, and NO_2 were 194, 17.2, and 8.02, respectively, which were significantly higher than those of other adsorption systems. This proves again that the Rh-GeSe monolayer has an obvious monitoring effect on SO_2, C_2H_2, and NO_2 gas molecules. This shows that the response of the Rh-GeSe monolayer to SO_2, C_2H_2, and NO_2 gas molecules is more prominent, and the conductivity changes greatly, which is enough to achieve the effect of gas detection, which is also consistent with the previous analysis.

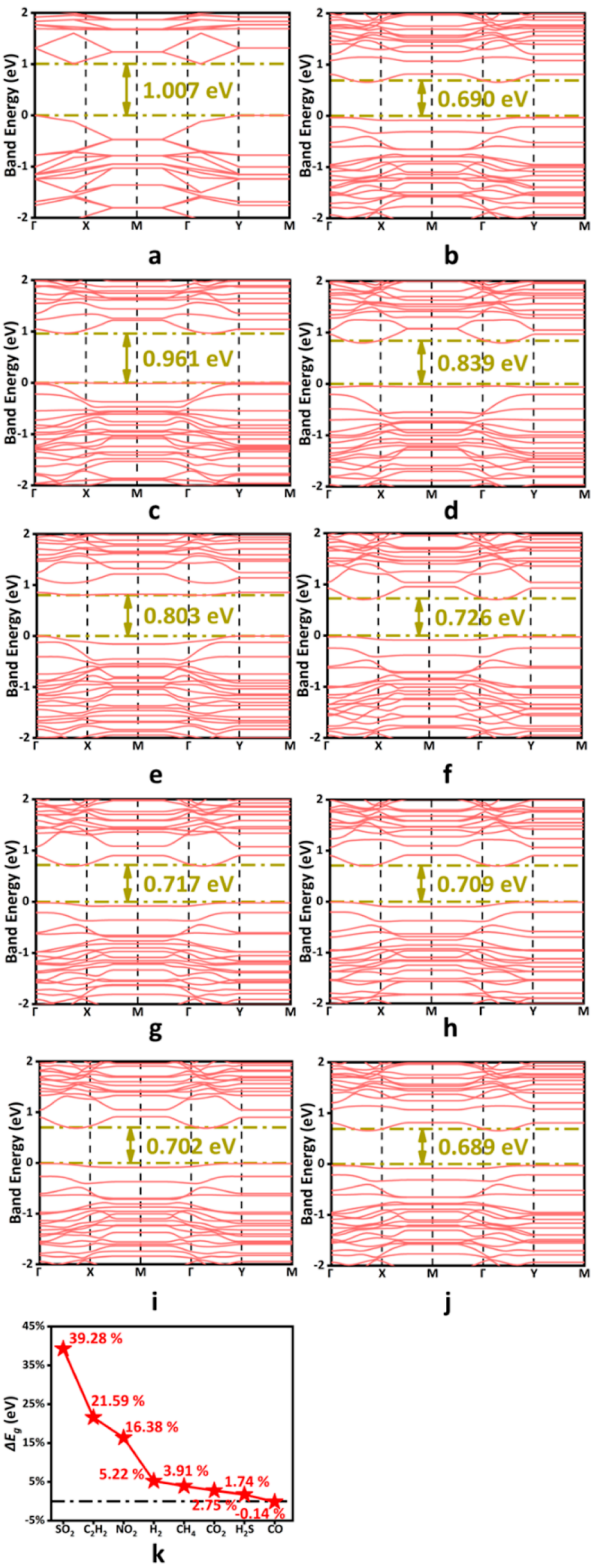

Figure 5. Band energy of (a) GeSe monolayer, (b) Rh-GeSe monolayer, (c) SO_2, (d) C_2H_2, (e) NO_2, (f) H_2, (g) CH_4, (h) CO_2, (i) H_2S, (j) CO adsorption systems, and (k) band gap energy changes (ΔE_g) of each adsorption system.

https://doi.org/10.1021/acsomega.3c09001
ACS Omega 2024, 9, 7061−7068

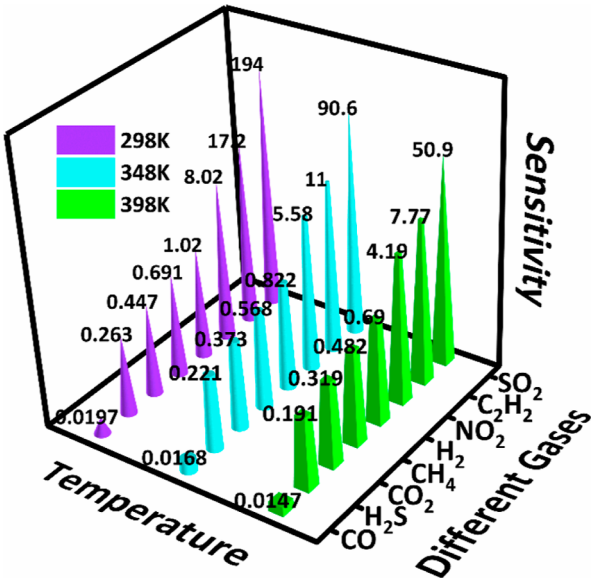

Figure 6. Sensitivity of SO_2, C_2H_2, NO_2, H_2, CH_4, CO_2, H_2S, and CO adsorption systems.

4. CONCLUSIONS

As an important part of sensor technology, gas sensor plays an indispensable role in the detection of toxic, harmful, and explosive gases and intelligent medical diagnosis. From life to industry, from the military to aerospace, all aspects are inseparable from the application of gas detection technology. Based on DFT, the models of Rh atom doped GeSe monolayer and eight target gases (SO_2, C_2H_2, NO_2, H_2, CH_4, CO_2, H_2S, CO) were constructed by Materials Studio software in this study, and the adsorption properties of each system were analyzed and calculated. By comparing the geometric structure, adsorption distance ($d_{sub/gas}$), binding energy (E_b), adsorption energy (E_{ads}), transfer charge (ΔQ), the DOS, band structure, ELF, CDD, and sensitivity (S) of different systems, the main conclusions are as follows:

1 There is no covalent bond between the gas molecule and the nearest atom (Rh) in Rh-GeSe, and there is no electronic localization overlap in the ELF image. The adsorption energies of the most stable adsorption systems of NO_2, C_2H_2, SO_2, H_2S, H_2, CH_4, CO_2, and CO are −2.009, −1.656, −1.630, −1.183, −0.817, −0.448, −0.308, and −0.059 eV, respectively. Among them, the adsorption of NO_2, C_2H_2, SO_2, H_2S, and H_2 is more likely to be between physical adsorption and chemical adsorption. The adsorption of CH_4, CO_2, and CO adsorption system is weak physical adsorption.
2 The transfer charge of the most stable SO_2, NO_2, H_2S, CH_4, H_2, CO_2, C_2H_2, CO adsorption systems are −0.405 e, −0.274 e, −0.22e, 0.164 e, 0.157 e, −0.142 e, 0.047 e, −0.001 e. In SO_2, NO_2, H_2S, CO_2, and CO adsorption systems, gas molecules act as electron acceptors and Rh-GeSe monolayer acts as an electron donor. In CH_4, H_2, and C_2H_2 adsorption systems, Rh-GeSe monolayer acts as electron acceptor and gas molecule acts as an electron donor.
3 From the perspective of TDOS, band structure, and response degree, Rh-GeSe monolayer has a prominent response to SO_2, C_2H_2, and NO_2 gas molecules, while it is insensitive to H_2, CH_4, CO_2, H_2S, and CO gas molecules, indicating that Rh-GeSe monolayer has a certain selectivity. Therefore, the Rh-GeSe monolayer has the potential to become an excellent gas sensing material.

AUTHOR INFORMATION

Corresponding Author

Liang-Yan Guo − *National Key Laboratory of Power Transmission Equipment Technology, School of Electrical Engineering, Chongqing University, Chongqing 400044, China;* orcid.org/0009-0006-1732-461X; Email: guoliangyan@cqu.edu.cn

Authors

Yunfeng Long − *Yunnan Key Laboratory of Green Energy, Electric Power Measurement Digitalization, Control and Protection, Electric Power Research Instute of Yunnan Power Grid Company, Limited, Kunming 650214 Yunnan, China;* orcid.org/0000-0001-7803-4022

Zhaoyu Peng − *Yunnan Key Laboratory of Green Energy, Electric Power Measurement Digitalization, Control and Protection, Electric Power Research Instute of Yunnan Power Grid Company, Limited, Kunming 650214 Yunnan, China*

Xiaohui He − *Yunnan Key Laboratory of Green Energy, Electric Power Measurement Digitalization, Control and Protection, Electric Power Research Instute of Yunnan Power Grid Company, Limited, Kunming 650214 Yunnan, China*

Mengyao Zhu − *Yunnan Key Laboratory of Green Energy, Electric Power Measurement Digitalization, Control and Protection, Electric Power Research Instute of Yunnan Power Grid Company, Limited, Kunming 650214 Yunnan, China*

Zewen Yang − *Yunnan Key Laboratory of Green Energy, Electric Power Measurement Digitalization, Control and Protection, Electric Power Research Instute of Yunnan Power Grid Company, Limited, Kunming 650214 Yunnan, China*

Taiwen Liu − *Yunnan Key Laboratory of Green Energy, Electric Power Measurement Digitalization, Control and Protection, Electric Power Research Instute of Yunnan Power Grid Company, Limited, Kunming 650214 Yunnan, China*

Complete contact information is available at: https://pubs.acs.org/10.1021/acsomega.3c09001

Author Contributions

Y.L. and Z.P. contributed equally to this work. Y.L. and L.-Y.G. conceived the original research idea, Z.P. and X.H. conceived the computational details, M.Z. and Z.Y. conceived the methodology, and T.L. conceived the analyses. The manuscript was written through the contributions of all authors. All authors have given approval to the final version of the manuscript.

Notes

The authors declare no competing financial interest.

ACKNOWLEDGMENTS

This work was supported by China Southern Power Grid Co., Ltd. Innovation Project YNKJXM20220009.

REFERENCES

(1) Abu Bakar, N.; Abu-Siada, A. A New Method to Detect Dissolved Gases in Transformer Oil Using NIR-IR Spectroscopy. *IEEE Trans. Dielectr. Electr. Insul.* **2017**, *24* (1), 409−419.

https://doi.org/10.1021/acsomega.3c09001
ACS Omega 2024, 9, 7061−7068

(2) Liu, Y.; Yang, Z.; Huang, L.; Zeng, W.; Zhou, Q. Anti-Interference Detection of Mixed NO_X via In_2O_3-Based Sensor Array Combining with Neural Network Model at Room Temperature. *J. Hazard. Mater.* **2024**, *463*, 132857.
(3) Chen, D.; Li, Y.; Xiao, S.; Yang, C.; Zhou, J.; Xiao, B. Single Ni Atom Doped WS2Monolayer as Sensing Substrate for Dissolved Gases in Transformer Oil: A First-Principles Study. *Appl. Surf. Sci.* **2022**, *579*, 152141.
(4) Peng, R.; Zeng, W.; Zhou, Q. Adsorption and Gas Sensing of Dissolved Gases in Transformer Oil onto Ru_3-Modified SnS_2: A DFT Study. *Appl. Surf. Sci.* **2023**, *615*, 156445.
(5) Chen, Y.; Zhang, W.; Zhang, S.; He, H.; Zhang, X. Sensing Response of Pd-Modified Ti3C2O2 for Dissolved Gas Molecules in Power Transformer Oil. *Mater. Today Commun.* **2023**, *34*, 105453.
(6) Zhao, P.; Tang, M.; Zhang, D. Adsorption of Dissolved Gas Molecules in the Transformer Oil on Metal (Ag, Rh, Sb)-Doped PdSe2Momlayer: A First-Principles Study. *Appl. Surf. Sci.* **2022**, *600*, 154054.
(7) Zhang, J.; Feng, W.; Zhang, Y.; Zeng, W.; Zhou, Q. Gas-Sensing Properties and First-Principles Comparative Study of Metal (Pd, Pt)-Decorated $MoSe_2$ Hierarchical Nanoflowers for Efficient SO_2 Detection at Room Temperature. *J. Alloys Compd.* **2023**, *968*, 172006.
(8) Zhu, H.; Chen, X.; Hong, Z.; Huang, X.; Meng, F.-B.; Awais, M.; Paramane, A. Ni-Doped Boron Nitride Nanotubes as Promising Gas Sensing Material for Dissolved Gases in Transformer Oil. *Mater. Today Commun.* **2022**, *33*, 104845.
(9) Chen, J.; Jia, L.; Cui, X.; Zeng, W.; Zhou, Q. Adsorption and Gas-Sensing Properties of SF_6 Decomposition Components (SO_2, SOF_2 and SO_2F_2) on Co or Cr Modified GeSe Monolayer: A DFT Study. *Mater. Today Chem.* **2023**, *28*, 101382.
(10) Badawi, M.; Ibrahim, S. A.; Mansour, D.-E. A.; El-Faraskoury, A. A.; Ward, S. A.; Mahmoud, K.; Lehtonen, M.; Darwish, M. M. F. Reliable Estimation for Health Index of Transformer Oil Based on Novel Combined Predictive Maintenance Techniques. *IEEE Access* **2022**, *10*, 25954−25972.
(11) Elele, U.; Nekahi, A.; Arshad, A.; Fofana, I. Towards Online Ageing Detection in Transformer Oil: A Review. *Sensors* **2022**, *22* (20), 7923.
(12) Aasi, A.; Javahersaz, R.; Mehdi Aghaei, S.; Panchapakesan, B. Novel Green Phosphorene as a Superior Gas Sensor for Dissolved Gas Analysis in Oil Transformers: Using DFT Method. *Mol. Simul.* **2022**, *48* (6), 541−550.
(13) John, R. A. B.; Ruban Kumar, A. A Review on Resistive-Based Gas Sensors for the Detection of Volatile Organic Compounds Using Metal-Oxide Nanostructures. *Inorg. Chem. Commun.* **2021**, *133*, 108893.
(14) Lu, D.; Huang, L.; Zhang, J.; Zhang, Y.; Feng, W.; Zeng, W.; Zhou, Q. Rh-and Ru-Modified InSe Monolayers for Detection of NH_3, NO_2, and SO_2 in Agricultural Greenhouse: A DFT Study. *ACS Appl. Nano Mater.* **2023**, *6* (15), 14447−14458.
(15) Tan, P.-H.; Hsu, C.-H.; Shen, Y.-C.; Wang, C.-P.; Liou, K.-L.; Shih, J.-R.; Lin, C. J.; Lee, L.; Wang, K.; Wu, H.-M.; Chiang, T.-Y.; Chih, Y.-D.; Chang, J.; King, Y.-C.; Chueh, Y.-L. Complementary Metal-Oxide-Semiconductor Compatible 2D Layered Film-Based Gas Sensors by Floating-Gate Coupling Effect. *Adv. Funct. Mater.* **2022**, *32* (13), 2108878.
(16) Staerz, A.; Weimar, U.; Barsan, N. Current State of Knowledge on the Metal Oxide Based Gas Sensing Mechanism. *Sens. Actuators, B* **2022**, *358*, 131531.
(17) Li, Y.-T.; Sun, K.; Luo, D.; Wang, Y.-M.; Han, L.; Liu, H.; Guo, X.-L.; Yu, D.-L.; Ren, T.-L. A Review on Low-Dimensional Novel Optoelectronic Devices Based on Carbon Nanotubes. *AIP Adv.* **2021**, *11* (11), 110701.
(18) Bartolome, J.; González, M.; Vázquez-López, A.; del Prado, F.; Tecedor, M.; Vasquez, G.; Ramírez-Castellanos, J.; Cremades, A.; Maestre, D. Low-Dimensional Structures of In2O3, SnO_2 and TiO_2 with Applications of Technological Interest. *Oxide-Based Materials and Structures*; CRC Press, 2020; pp 99−136.
(19) Guo, L.-Y.; Zhao, J.; Guo, J.; Song, Y.; Jiang, P.; Jiang, T.; Huang, Z. Highly Sensitive Gas Sensors Based on Ag-doped SnS Monolayer for NO_2 and NO Harmful Gases Detection. *IEEE Sens. J.* **2023**, 1.
(20) Tien, N. T.; Bich Thao, P. T.; Phuc, V. T.; Ahuja, R. Influence of Edge Termination on the Electronic and Transport Properties of Sawtooth Penta-Graphene Nanoribbons. *J. Phys. Chem. Solids* **2020**, *146*, 109528.
(21) Guo, L.-Y.; Xia, S.-Y.; Tan, Y.; Huang, Z. Zr-Doped h-BN Monolayer: A High-Sensitivity Atmospheric Pollutant-Monitoring Sensor. *Sensors* **2022**, *22* (11), 4103.
(22) Guo, L.-Y.; Xia, S.-Y.; Long, Y.; Peng, Z.; Tan, Y.; Jiang, T.; Huang, Z. P-Doped h-BN Monolayer: A High-Sensitivity SF_6 Decomposition Gases Sensor. *IEEE Sens. J.* **2022**, *22* (19), 18281−18286.
(23) Lu, D.; Zhang, Y.; Feng, W.; Zeng, W.; Zhou, Q. Experimental and Theoretical Comparative Analysis of Modified Graphene (G-O, Pd-G, Pd-G-O) Sensing Performance toward SO_2 in Agricultural Greenhouse. *Ceram. Int.* **2023**, *49* (16), 26516−26529.
(24) Ashraf, N.; Isa khan, M.; Majid, A.; Rafique, M.; Tahir, M. A Review of the Interfacial Properties of 2-D Materials for Energy Storage and Sensor Applications. *Chin. J. Phys.* **2020**, *66*, 246−257.
(25) Guo, L.-Y.; Xia, S.-Y.; Sun, H.; Li, C.-H.; Long, Y.; Zhu, C.; Gui, Y.; Huang, Z.; Li, J. A DFT Study of the Ag-Doped h-BN Monolayer for Harmful Gases (NO2, SO2F2, and NO). *Surface. Interfac.* **2022**, *32*, 102113.
(26) Chen, J.; Chen, J.; Zeng, W.; Zhou, Q. Adsorption of HCN on WSe2Monolayer Doped with Transition Metal (Fe, Ag, Au, As and Mo). *Sens. Actuators, A* **2022**, *341*, 113612.
(27) Rani, S.; Kumar, M.; Garg, P.; Parmar, R.; Kumar, A.; Singh, Y.; Baloria, V.; Deshpande, U.; Singh, V. N. Temperature-Dependent n-p-n Switching and Highly Selective Room-Temperature n-SnSe2/p-SnO/n-SnSe Heterojunction-Based NO2 Gas Sensor. *ACS Appl. Mater. Interfaces* **2022**, *14* (13), 15381−15390.
(28) Afzal, A. M.; Iqbal, M. Z.; Dastgeer, G.; Nazir, G.; Mumtaz, S.; Usman, M.; Eom, J. WS2/GeSe/WS2 Bipolar Transistor-Based Chemical Sensor with Fast Response and Recovery Times. *ACS Appl. Mater. Interfaces* **2020**, *12* (35), 39524−39532.
(29) Wang, B.; Gu, Y.; Chen, L.; Ji, L.; Zhu, H.; Sun, Q. Gas Sensing Devices Based on Two-Dimensional Materials: A Review. *Nanotechnology* **2022**, *33* (25), 252001.
(30) Tao, L.-Q.; Wang, G.; Hou, P.; Liu, J.; Chen, X. Physisorption behaviors of deoxyribonucleic acid nucleobases and base pairs on bismuthene from theoretical insights. *Appl. Surf. Sci.* **2023**, *627*, 157242.
(31) Zhang, D.; Yu, S.; Wang, X.; Huang, J.; Pan, W.; Zhang, J.; Meteku, B. E.; Zeng, J. UV Illumination-Enhanced Ultrasensitive Ammonia Gas Sensor Based on (001) TiO2/MXene Heterostructure for Food Spoilage Detection. *J. Hazard. Mater.* **2022**, *423*, 127160.
(32) Tang, M.; Wang, Z.; Wang, D.; Mao, R.; Zhang, H.; Xu, W.; Yang, Z.; Zhang, D. Construction of LaF_3QD-Modified SnS_2 Nanorod Composites for Ultrasensitive Detection of H_2S. *J. Mater. Chem. A* **2023**, *11* (18), 9942−9954.
(33) Tang, M.; Zhang, D.; Wang, D.; Deng, J.; Kong, D.; Zhang, H. Performance Prediction of 2D Vertically Stacked MoS_2-WS_2 Heterostructures Base on First-Principles Theory and Pearson Correlation Coefficient. *Appl. Surf. Sci.* **2022**, *596*, 153498.
(34) Ma, Z.; Shi, W.; Yan, K.; Pan, L.; Yu, G. Doping Engineering of Conductive Polymer Hydrogels and Their Application in Advanced Sensor Technologies. *Chem. Sci.* **2019**, *10* (25), 6232−6244.
(35) Lee, S. H.; Eom, W.; Shin, H.; Ambade, R. B.; Bang, J. H.; Kim, H. W.; Han, T. H. Room-Temperature, Highly Durable $Ti_3C_2T_{<i>x</i>}$ MXene/Graphene Hybrid Fibers for NH_3 Gas Sensing. *ACS Appl. Mater. Interfaces* **2020**, *12* (9), 10434−10442.
(36) Zhang, L.; Zhou, Y.; Han, S. The Role of Metal-Organic Frameworks in Electronic Sensors. *Angew. Chem.* **2021**, *133* (28), 15320−15340.

https://doi.org/10.1021/acsomega.3c09001
ACS Omega 2024, 9, 7061−7068